Multicomponent Organization Analysis in Spatial Domains of Atrial Fibrillation

Francisco M. Melgarejo-Meseguer[1], Amanda Román-Román[1], Javier Gimeno-Blanes[2], Sergio Muñoz-Romero[1], Arcadi García-Alberola[3], Juan José Sánchez-Muñoz[3], Omer Berenfeld[4], José Luis Rojo-Álvarez[1]
[1] Universidad Rey Juan Carlos, Spain. [2] Universidad Miguel Hernández (Spain). [3] Hospital Clínico Universitario Virgen de la Arrixaca de Murcia (Spain). [4] University of Michigan, USA

Abstract

Atrial fibrillation (AF) is a common heart rhythm disorder associated with elevated health risks. This study introduces an innovative approach utilizing regression models to identify regions of tissue in the heart linked to AF. The research involved examining the frequency characteristics of various areas in the heart prone to arrhythmias and employing an elastic net regression (ENR) technique to pinpoint significant frequency contributions. This process led to the creating of three-dimensional (3D) maps illustrating the likelihood of arrhythmia origins. We evaluated the effectiveness of our method by applying it to both two-dimensional (2D) and 3D AF simulations and comparing the results with those obtained using least-squares (LS) algorithms. The findings underscored the advantages of ENR. The simulations successfully identified stable rotor and wavebreak regions, though some harmonic frequencies were not captured. We observed clearly defined regional maps in normal atrial tissue, with notable harmonics occurring at 5.9 Hz in the left atrium. In contrast, the right atrium displayed a smaller rotor region with some missed harmonic frequencies. In fibrotic left atrial substrates, harmonics at 7.8 Hz were consistently detected. Using multi-component domains allowed for a comprehensive analysis based on harmonically related components. Different estimation methods produced comparable results, facilitating the localization of spatial regions containing AF sources despite a moderate loss of harmonic frequencies.

1. Introduction

Cardiovascular diseases are the leading cause of global mortality, accounting for approximately 17.7 million deaths in 2015, which represents nearly 31% of all recorded fatalities worldwide. This group of diseases includes cardiovascular ischemia, arrhythmias, aneurysms, and heart failure. Atrial fibrillation (AF) is a prevalent arrhythmia affecting about 1-2% of the global population [1]. AF is classified as a supraventricular tachyarrhythmia characterized by abnormal contractions originating in the atria, resulting in a faster-than-usual sinus rhythm. The treatment options for AF include pharmaceutical remedies and surgical interventions. According to [2], ablation is recommended as a secondary treatment if the pharmaceutical approach fails to produce the desired outcomes. Ablation involves using energy to eliminate or destroy the abnormal cardiac tissue responsible for causing AF. Despite several proposed theories, the exact cause of AF remains unknown. One theory, known as the rotor theory [3], suggests that AF originates from spiral-shaped re-entries called rotors. These rotors occur when an electrical impulse re-enters an unintended location within the heart, contributing to the development of tachyarrhythmias.

Various computational mapping analysis tools have been developed to visualize the cardiac electrical activation and identify the rotors sustaining fibrillation. Once these rotors are identified, clinicians can ablate to eliminate AF. Spatial frequency characterization maps have been utilized in AF analysis to visualize the cardiac electrical activity. This approach helps identify the specific area requiring ablation [4, 5]. Frequency characterization involves analyzing the spectral content of the signals. Spectral analysis is preferred over temporal analysis due to the presence of regularity and patterns in AF, as opposed to the low level of organization observed in temporal analysis [6]. Spatial characterization involves examining the location and distribution of signals. In the context of AF, spatial frequency characterization is employed to understand its spatial distribution and frequency characteristics.

The current study focuses on domain segmentation, which entails identifying and delineating specific areas associated with the AF organization. Relevant domains of interest include the rotor and wavebreak domains, which exhibit different frequencies than the contacting rotor.

The article is structured as follows: Section 2 comprehensively explains the materials used, encompassing simulations and real two- and three-dimensional signals. It also

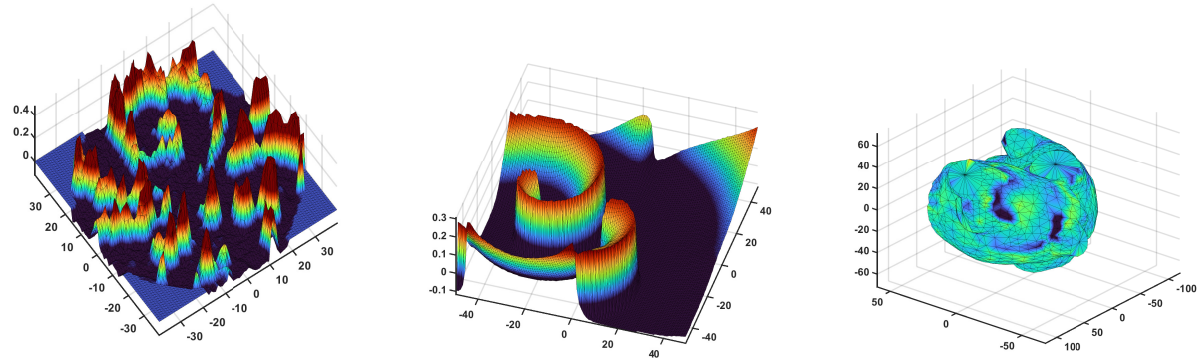

(a) (b) (c)

Figure 1. Rotor regions for each presented case: (a) Optical map of rat ventricular myocardium; (b) 2D simulation depicting a rotor; (c) 3D simulation exhibiting fibrosis and an AF focus in the left atrium.

outlines the analysis methods employed, such as Fourier Organizational Analysis (FOA) and elastic net regression (ENR). Section 3 presents the tests conducted using simulated AF data and real cases to evaluate the various estimators discussed earlier. Finally, Section 4 summarizes the main results, contributions, and potential future research directions.

2. Materials and Methods

This section provides an overview of the dataset, including real 2D signals and 2D/3D simulations. It also introduces the signal model used for determining significant spectral frequencies and explains the role of probability maps in identifying distinct regions in cardiac tissue.

Datasets. First, we used a collection of data comprising real 2D signals, 2D simulations, and 3D simulations. The real 2D signals, shown in Figure 1(a), were obtained using optical mapping techniques. These signals were acquired from a study investigating the role of the hERG potassium channel in generating cardiac arrhythmias in neonatal rat ventricular myocardial cells [7]. The sampling frequency varies, with one case recorded at 50 Hz and the others at 33 Hz. Each case consists of 6400 data points, but the low sampling rate poses challenges for video analysis due to the moderate resolution. Second, a 2D simulation was conducted, as depicted in Figure 1(b), to test the hypothesis that highly periodic waves originating from AF sources in or near the posterior left atrium result in increased fragmented activity in neighboring regions [8]. The simulations were performed at a sampling frequency of 1 kHz, and each simulation comprises 2048 data points. Finally, a 3D simulation was included, shown in Figure 1(c), as part of a thesis aimed at assessing the non-invasive estimation of dominant epicardial regions with high-frequency characteristics during AF [9]. The simulations were conducted with a sampling frequency of 500 Hz, and each simulation consisted of 10,000 data points. The case used in this simulation involves the presence of fibrosis alongside an AF focus in the left atrium.

Signal Model and Domain Maps. Concerning the signal model, we proposed a method for determining the most significant spectral frequencies according to the FOA previously proposed for ECG signals. This model aims to identify different regions in the cardiac tissue in terms of different spectral contents and organization. The spectral regions are represented using spatial probability maps, which assist in quantifying the presence of each domain.

As detailed in [10], the FOA signal model for a cardiac signal $s(t)$ is given by projecting the measured signal onto the following signal model:

$$\hat{s}(t|f_0) = \sum_{k=1,+,-}^{K} A_k cos\left(2\pi k f_0^{(+,-)} + \phi_k\right) \qquad (1)$$

where A_k, ϕ_k denote the amplitude and acrophases or the harmonic components of fundamental frequency f_0, and the notation $(+,-)$ indicates that similar terms are included for fluctuations in $f_0 + \Delta f$ and in $f_0 - \Delta f$, respectively (see reference for details). Note that the estimation is conditional to choosing an adequate fundamental frequency f_0.

If we assume that different fundamental frequencies can be associated with different underlying activation patterns in the cardiac substrate, we can assume the cardiac signal consists of the contributions of those patterns, this is,

$$s(t) \simeq \hat{s}(t) = \sum_{q=1}^{Q} \hat{s}\left(t|f_0^{(q)}\right) \qquad (2)$$

We can obtain the set of amplitudes and phases using Least Squares Spectral Analysis (LSSA) by applying LS

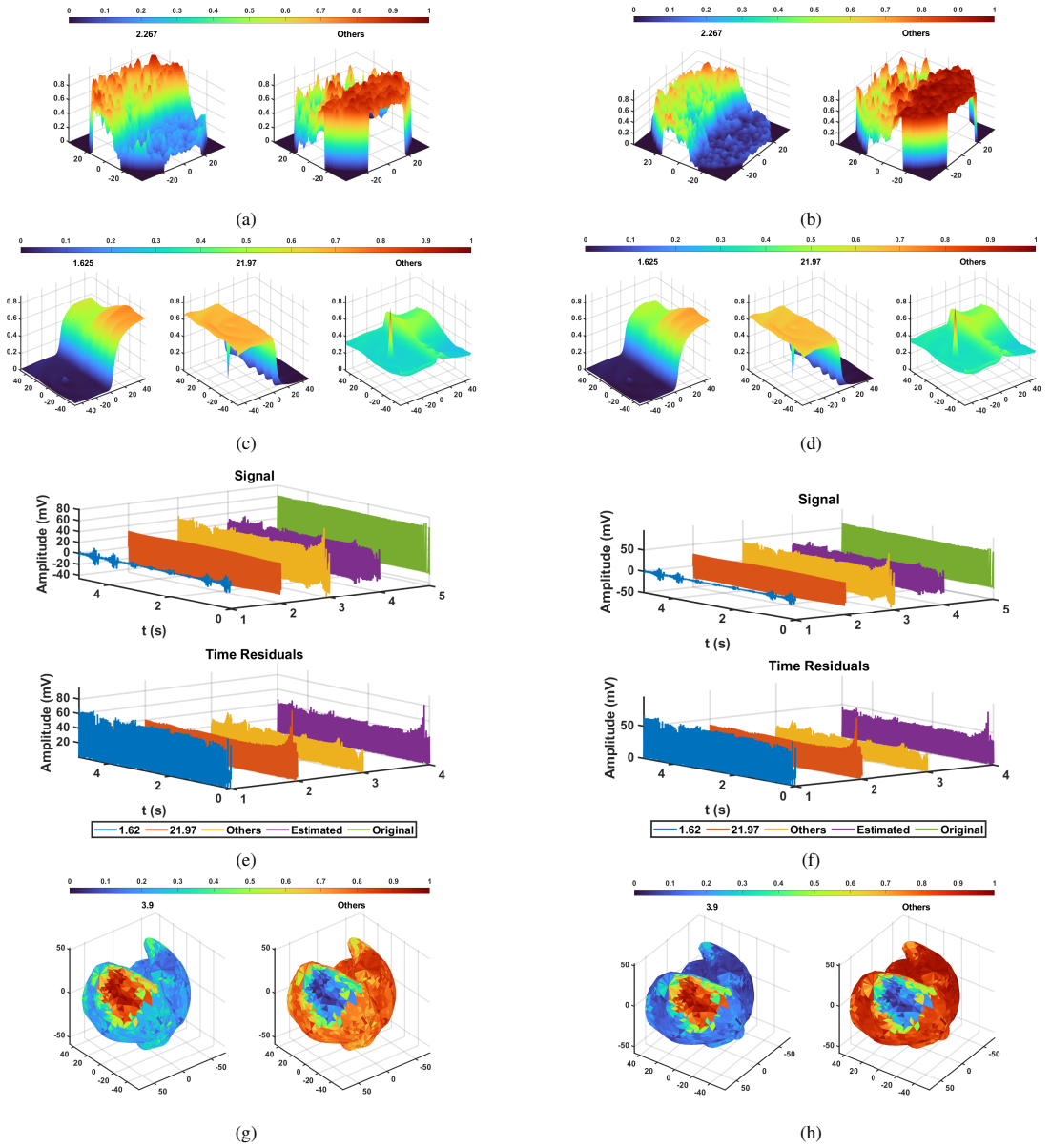

Figure 2. Frequency maps computed using LS and ENR methods across various cases. LS and ENR frequency maps are presented in (a) and (b) for the optical mapping case and in (c) and (d) for the planar cardiac tissue simulation case. The upper panel of (e) and (f) represents the signal estimation for selected frequencies in blue and orange, the signal for remaining frequencies in yellow, the combined estimated signal in purple, and the original signal in green, applicable to both LS and ENR methods. The lower panel of (e) and (f) showcases residuals for the estimated signal of selected frequencies in blue and orange, residuals computed with the remaining frequencies in yellow, and residuals for the estimated signal created by combining the selected frequencies. Finally, (g) and (h) display the frequency maps for 3D fibrotic atria simulation registration computed by LS and ENR, respectively.

to a signal model in a grid of frequencies. LSSA is a form of spectral analysis that fits a model to the signal using linear regression, and it uses amplitude and phase values at each frequency in the grid. However, the approach described in this article deviates from conventional LSSA by using a frequency selection strategy instead of a predefined frequency range. The selected frequencies, their harmonics, and nearby fluctuations are chosen based on specific criteria and regions of interest within the signal. The LS method cannot always deal with limited observations or situations where the number of samples is comparable with the number of free parameters of the model.

To address stability concerns, penalized linear regression techniques, such as ridge regression (L2 penalty) and LASSO (L1 penalty), can be used. Ridge regression reduces coefficient magnitudes, while LASSO allows for variable selection by shrinking certain coefficients to zero. ENR combines both L1 and L2 penalties, offering a balance between variable selection and coefficient regularization, and this method solves an optimization problem to determine the coefficients.

For a set of signals measured in different spatial locations at a given cardiac surface S, this is, $\bar{r}_i \in \bar{r}_S$, this data model is estimated in each spatial location, i.e.,

$$s(t,\bar{r}_S) = \hat{s}(t,\bar{r}_S) + e(t,\bar{r}_S) = \sum_{q=1}^{Q} \hat{s}(t|f_0^{(q)},\bar{r}_S) + e(t,\bar{r}_S) \quad (3)$$

For yielding probability maps, we can take energy ratios at each location and then,

$$p(f_0^{(q)},\bar{r}_S) = \frac{\|\hat{s}(t|f_0^{(q)},\bar{r}_S)\|^2}{\|s(t,\bar{r}_S)\|^2} \quad (4)$$

where p is the normalized power contributed by dominant frequency f_0^q as a function of surface location $\bar{r}_S$.

3. Experiments and Results

The experimental procedure can be outlined as follows: Initially, a thorough examination of the signals was conducted to identify specific regions of interest, such as rotors or wavebreaks. Subsequently, the frequencies to be analyzed were manually chosen based on the signal spectrum. Finally, the probability maps and reconstruction errors were computed.

Figure 2 shows a compendium of results. In the simulated data, the probability maps exhibited well-defined spatial distributions, with smooth transitions in the interface, and the core showed a different distribution from both substrate regions. The optical mapping recordings also showed well-defined spatial regions, although with more spatial with-in region fluctuations. Finally, the surface simulation showed connected and compact regions in the reentry and surroundings and outside it. In the optical mapping and the simulations, ENR method presented less spatial blurring and fluctuations than the LS estimator.

4. Conclusions

The generalization of FOA method to a spatial diversity of signals can provide compact domains. ENR method can yield better solutions in terms of in-domain blurring. These results can be advanced in order to support clinicians in understanding AF mechanisms and establishing ablation targets.

Acknowledgements

Partially supported by the Ministry of Economy and Competitiveness, grant IPT-2012-1126- 300000, AEI/10.13039/5011000110033-PID2019-106623RB, AEI/ 10.13039/ 5011000110033 PID2019-104356RB, AEI / 10.13 039/ 5011000110033- PID2022-140786NB-C31, 2022 -REGING-95982, and 2022-REGING-92049. Partially funded by the Autonomous Community of Madrid for ELLIS Society (Madrid node).

References

[1] Gómez-Doblasa JJ, López-Garido MA, et al. Epidemiology of atrial fibrillation. Revista Española de Cardiologia English Edition 2016;16(A):2–7.

[2] Knuuti J, Wijns W, et al. Guía ESC 2020 sobre diagnóstico y tratamiento de la cardiopatía isquémica crónica. Revista Española de Cardiologia 2020;73(10):801–899.

[3] Guillem MS, Climent AM, Rodrigo M, Fernández-Avilés F, Atienza F, Berenfeld O. Presence and stability of rotors in atrial fibrillation: evidence and therapeutic implications. Cardiovascular Research 2016;109(4):480–492.

[4] Sanders P, Berenfeld O, Hocini M. Spectral analysis identifies sites of high-frequency activity maintaining atrial fibrillation in humans. ACC Current Journal Review 12 2005; 14:40.

[5] Atienza F, Almendral J, Jalife J, Zlochiver S, Ploutz-Snyder R, Torrecilla EG, Arenal A, Kalifa J, Fernández-Avilés F, Berenfeld O. Real-time Dominant Frequency Mapping and Ablation of Dominant Frequency Sites in Atrial Fibrillation with Left-to-right Frequency Gradients Predicts Long-term Maintenance of Sinus Rhythm. Heart Rhythm 2011; 8(11):1758–65.

[6] Berenfeld O, Ennis S, Hwang E, Hooven B, Grzeda K, Mironov S, Yamazaki M, Kalifa J, Jalife J. Time- and frequency-domain Analyses of Atrial Fibrillation Activation Rate: The Optical Mapping Reference. Heart Rhythm 2011;8(11):1758–65.

[7] Hou L, Deo M, et al. A major role for hERG in determining frequency of reentry in neonatal rat ventricular myocyte monolayer. Circulation Research 2010; 107(12):1503–1511.

[8] Kalifa J, Tanaka K, et al. Mechanisms of wave fractionation at boundaries of high-frequency excitation in the posterior left atrium of the isolated sheep heart during atrial fibrillation. Circulation 2006;113(5):626–633.

[9] Pedrón-Torrecilla J, Bort M, et al. Noninvasive estimation of epicardial dominant high-frequency regions during atrial fibrillation. Journal of Cardiovascular Electrophysiology 2016;27(4):435–442.

[10] Barquero-Pérez O, Rojo-Álvarez JL, Caamaño AJ, Goya-Esteban R, Everss E, Alonso-Atienza F, Sánchez-Muñoz JJ, García-Alberola A. Fundamental frequency and regularity of cardiac electrograms with fourier organization analysis. IEEE Transactions on Biomedical Engineering 2010; 57(9):2168–2177.